Phospholipase C β3 deficiency leads to macrophage hypersensitivity to apoptotic induction and reduction of atherosclerosis in mice

Zhenglong Wang,[1,2] Bei Liu,[3] Ping Wang,[1] Xuemei Dong,[1] Carlos Fernandez-Hernando,[1] Zhong Li,[2] Timothy Hla,[4] Zihai Li,[3] Kevin Claffey,[4] Jonathan D. Smith,[5] and Dianqing Wu[1]

[1]Program for Vascular Biology and Therapeutics and Department of Pharmacology, Yale University School of Medicine, New Haven, Connecticut, USA. [2]Department of Genetics and Developmental Biology, [3]Department of Immunology, and [4]Center for Vascular Biology, University of Connecticut Health Center, Farmington, Connecticut, USA. [5]Department of Cell Biology, Cleveland Clinic Foundation, Cleveland, Ohio, USA.

Atherosclerosis is an inflammatory disease that is associated with monocyte recruitment and subsequent differentiation into lipid-laden macrophages at sites of arterial lesions, leading to the development of atherosclerotic plaques. PLC is a key member of signaling pathways initiated by G protein–coupled ligands in macrophages. However, the role of this enzyme in the regulation of macrophage function is not known. Here, we studied macrophages from mice lacking PLC β2, PLC β3, or both PLC isoforms and found that PLC β3 is the major functional PLC β isoform in murine macrophages. Although PLC β3 deficiency did not affect macrophage migration, adhesion, or phagocytosis, it resulted in macrophage hypersensitivity to multiple inducers of apoptosis. PLC β3 appeared to regulate this sensitivity via PKC-dependent upregulation of Bcl-XL. The significance of PLC β signaling in vivo was examined using the apoE-deficient mouse model of atherosclerosis. Mice lacking both PLC β3 and apoE exhibited fewer total macrophages and increased macrophage apoptosis in atherosclerotic lesions, as well as reduced atherosclerotic lesion size when compared with mice lacking only apoE. These results demonstrate what we believe to be a novel role for PLC activity in promoting macrophage survival in atherosclerotic plaques and identify PLC β3 as a potential target for treatment of atherosclerosis.

Introduction

PLC hydrolyzes phosphatidylinositol 4,5–bisphosphate to generate 2 second messengers, inositol 1,3,4–triphosphate and diacylglycerol. While inositol 1,3,4-triphosphate regulates Ca^{2+} efflux, it and diacylglycerol activate PKC (1). The β family of PLC, which consists of 4 isoforms, PLC β1–β4, is regulated by heterotrimeric G proteins (2). PLC β2 is primarily expressed in hematopoietic cells, whereas PLC β3 and PLC β1 are expressed in a wide range of cells and tissues (2). PLC β4 is predominantly expressed in neuronal cells (3, 4). While all of the PLC β isoforms can be activated by the members of the Gq family of α subunits, PLC β2 and β3 can also be potently activated by Gβγ (5).

Macrophages are a heterogeneous population of leukocytes present ubiquitously in various tissues of the body. They are derived from monocytes after monocytes leave blood vessels. The heterogeneity of macrophages is shaped by the diverse microenvironments in which these cells are found. Macrophages have a role in regulating a wide range of homeostatic, immunological, and inflammatory processes (6, 7). One of the important biological functions of macrophages is host defense against microbial infections. Macrophages perform this duty by nonspecific killing through capturing and engulfing microbes and/or activating specific lymphocyte-based immune responses through antigen presentation and cytokine production. In addition to host defense, macrophages are inseparably associated with inflammation and particularly chronic inflammation, which is now believed to underlie many human diseases including atherosclerosis. Atherosclerosis is an inflammatory disease potentiated by overrecruitment of leukocytes — particularly monocytes/macrophages — into an arterial lesion (8–13). Oxidized LDL (oxLDL), among many possible triggers, has been identified as an initial inducer of endothelial cell and SMC dysfunction. These dysfunctional cells produce proinflammatory cytokines including chemokines, which, together with increased adhesiveness of endothelial cells, recruit monocytes to the intima. These monocytes then become macrophages, whose phagocytic activity allows the macrophages to become hyperlipidemic foam cells, the building blocks for atherosclerotic plaques. The foam cells eventually undergo apoptosis and produce more proinflammatory cytokines and chemokines that lead to recruitment of more monocytes. This process is one of the key pathogenic bases for the initiation and progression of atherosclerosis.

Studies using mice lacking monocyte chemoattractant protein 1 (MCP-1) or its receptor CCR2 provided strong genetic evidence for the involvement of chemokines in the pathogenesis of atherosclerosis (14, 15). When these mice were fed a high-fat diet (HFD), there was a decrease in atherosclerotic lesion size and a reduction in the number of infiltrated macrophages in the lesion (14, 15). This conclusion was further supported by a number of follow-up studies (16–21). In addition to MCP-1, other chemokines and

Nonstandard abbreviations used: CHX, cycloheximide; HFD, high-fat diet; LPA, lysophosphatic acid; MCP-1, monocyte chemoattractant protein 1; oxLDL, oxidized LDL; PAF, platelet-activating factor; SDF-1, stromal cell–derived factor 1; S1P, sphingosine 1–phosphate.

Conflict of interest: The authors have declared that no conflict of interest exists.

Citation for this article: *J. Clin. Invest.* **118**:195–204 (2008). doi:10.1172/JCI33139.

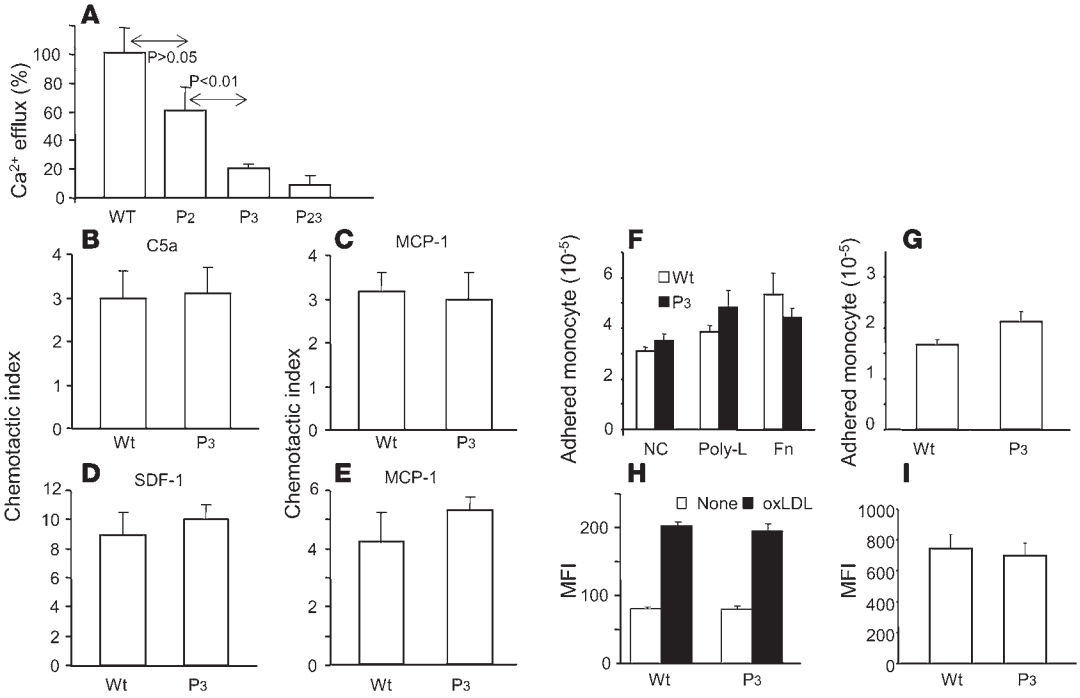

Figure 1

Effects of PLC β3 deficiency on macrophage functions. (**A**) Calcium effluxes induced by 10 nM C5a in macrophages isolated from wild-type mice and mice lacking PLC β2 (P_2), PLC β3 (P_3), or both (P_{23}). (**B**–**E**) Transendothelial migration of peritoneal macrophages and spleen monocytes. Peritoneal macrophages (**B** and **C**) or splenocytes (**D** and **E**) were added to the top chambers of Transwell plates precoated with mouse endothelial cells. C5a (10 nM), SDF-1 (100 ng/ml), or MCP-1 (60 ng/ml) were added to the lower chambers. After 4-hour incubation, cells in the lower chambers were collected, counted, and analyzed by FACS after staining with F4/80 (**B** and **C**) or CD11b/Gr1 (**D** and **E**) antibodies. The indices were calculated by dividing the number of F4/80-positive (**B** and **C**) or Gr-1^{lo}CD11b^{mid} (**D** and **E**) cells in the presence of ligand by that in its absence. $n = 8$; $P > 0.05$ for all **B**–**E**. (**F** and **G**) Adhesion of spleen monocytes to extracellular matrices and endothelial cells. Spleen cells were added onto 24-well plates without coating or coated with poly-lysine, fibronectin (**F**), or mouse endothelial cells (**G**). After 10 minutes, attached cells were collected, counted, and analyzed by FACS for Gr-1^{lo}CD11b^{mid} monocytes. $n = 4$; $P > 0.05$ for **F** and **G**. (**H**) Macrophage phagocytosis. Peritoneal macrophages were seeded on 24-well culture plates. Uncoated and oxLDL-coated FluoSphere beads were added to the cells. After extensive washes, cells were detached, stained with F4/80, and analyzed by FACS. $n = 4$; $P > 0.05$ between genotypes. (**I**) Uptake of apoptotic Jurkat cells. Macrophages were incubated with CFDA SE–labeled apoptotic Jurkat cells, detached, stained with a macrophage marker F4/80, and analyzed by FACS. The MFI of CFDA SE associated with F4/80-positive cells was determined. $n = 4$; $P > 0.05$. fn, fibronectin.

chemokine receptors have also been demonstrated to contribute to the initiation and progression of atherosclerotic lesion (9, 12). However, there is a lack of study of roles of signaling pathways activated by chemokines in atherogenesis, except for the recent study of PI3Kγ (22). Chemokines bind to their specific G protein–coupled receptors and regulate a number of signaling pathways that include PLC, PI3K, MAPKs, the Rho family of small GTPases, and adenylyl cyclases (23–25).

We have previously generated mice lacking PLC β2, PLC β3, and both and found that chemokines use both PLC β isoforms in mouse neutrophils, even though PLC β2 appeared to be the predominant isoform (26, 27). Although neutrophils lacking both PLC β2 and PLC β3 produced no Ca^{2+} efflux in response to fMLP or IL-8, potent neutrophil chemoattractants, no significant chemotactic defects were found with these neutrophils using Transwell assays (26, 27). This suggests that PLC signaling may be dispensable in cell migration. Macrophages, like neutrophils, also respond to certain chemokines (MCP-1 and stromal cell–derived factor 1 [SDF-1], for instance) and other G protein-coupled ligands (lysophosphatic acid [LPA] and sphingosine 1–phosphate [S1P], for instance) to produce Ca^{2+} efflux via activation of PLC. In this study, we investigate the role of PLC β2 and PLC β3 in G protein–coupled ligand–induced PLC activation and the role of PLC signaling in macrophage responses and in vivo functions.

Results

To investigate whether PLC β2 or PLC β3 is involved in chemoattractant-induced PLC activity in macrophages, we examined C5a-induced Ca^{2+} efflux in peritoneal macrophages isolated from wild-type, PLC β2–null, PLC β3–null, and PLC β2/β3–double-null mice. As shown in Figure 1A and Supplemental Figure 1 (supplemental material available online with this article; doi:10.1172/JCI33139DS1), PLC β3 deficiency led to a greater reduction in C5a response than PLC β2 deficiency, and PLC β2/β3 double deficiency almost abolished C5a-induced Ca^{2+} efflux. We also measured responses to a number of other G protein–coupled ligands, including SDF-1, MCP-1, platelet-activating factor (PAF), LPA, and S1P. Similar results were observed (data not shown). These data together indicate that although both PLC β2 and PLC β3 are required for G protein–coupled ligand–induced PLC activation, PLC β3 is the major functional isoform in these macrophages.

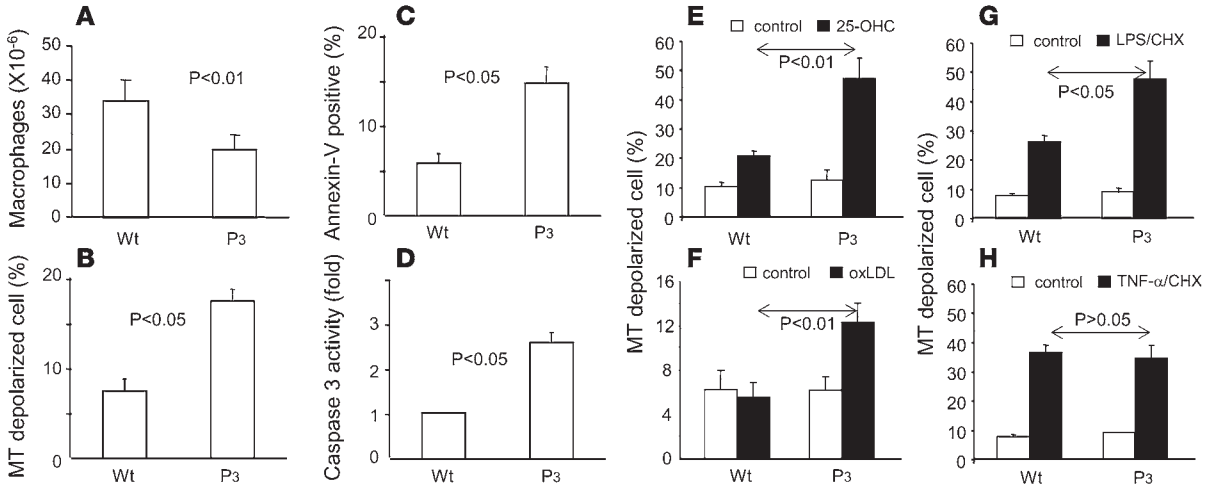

Figure 2

PLC β3 deficiency leads to an increased sensitivity of macrophages to apoptosis induction. (**A**–**D**) Increased apoptosis in macrophages from the 3-day thioglycolate-elicited model. (**A**) The numbers of peritoneal macrophages recovered from mice injected with thioglycolate for 3 days were counted (n = 27). (**B**) Percentages of macrophages with depolarized mitochondria (n = 4) were determined by FACS with the Mito-Probe dye and the anti-F4/80 antibody. (**C**) Percentages of annexin V–positive macrophages (n = 5) were determined by FACS analysis with annexin V and F4/80 antibodies. (**D**) Caspase-3 activity (n = 5) was determined using a caspase-3 assay kit from Roche Inc. (**E**–**H**) Increased sensitivity to apoptotic induction in macrophages from the 1-day thioglycolate–elicited model. Mice were injected with thioglycolate for 1 day, and percentages of macrophages with depolarized mitochondria (n > 4) were determined by FACS. For treatments, cells were incubated with 10 μg/ml 25-OHC, 100 μg/ml oxLDL, LPS (1 μg/ml)/CHX (1 μg/ml), or TNF-α (10 ng/ml)/CHX (10 μg/ml) for 24 hours. MT, mitochondria.

Next, we investigated the significance of PLC β3–mediated signaling in regulation of cellular responses of macrophages and monocytes, the precursors of macrophages, which include migration, adhesion, phagocytosis, and apoptosis. The effects of PLC β3 deficiency on macrophage chemotaxis in response to MCP-1 and C5a were examined using the Transwell migration assay. No significant effects were observed on macrophage migration through either a bare polycarbon membrane (data not shown) or mouse endothelial cells (Figure 1, B and C). We also examined the migration of monocytes in response to SDF-1 and MCP-1, and no significant differences between wild-type and PLC β3–deficient spleen monocytes were observed in the transendothelial Transwell assay (Figure 1, D and E). We next examined the effects of PLC β3 deficiency on monocyte adhesion. Spleen monocytes from wild-type and PLC β3–null mice showed the same ability to adhere to the uncoated surface or surfaces coated with poly-lysine or fibronectin (Figure 1F). These monocytes also showed the same adherence to mouse endothelial cells (Figure 1G). In addition, PLC β3 deficiency did not appear to affect the ability of macrophages to uptake uncoated or oxLDL-coated FluoSphere beads (Figure 1H), nor did it affect the engulfment of anti-Fas antibody–induced apoptotic Jurkat cells (Figure 1I). Putting these results together, we believe that PLC β3 deficiency does not appear to causes significant alterations in migration, adhesion, phagocytosis, or uptake of oxLDL or apoptotic cells.

When we isolated macrophages for the aforementioned functional studies from the peritonea of mice injected with thioglycolate for 3 days, we noticed that there was a statistically significant reduction in the number of macrophages from PLC β3–null mice compared with wild-type mice (Figure 2A). Given that there were no differences in macrophage/monocyte migration and adhesion, the difference in cell number suggests that PLC β3–mediated signaling may be involved in regulation of macrophage survival. We went on examining whether there were more apoptotic macrophages in these preparations using annexin V and Mito-Probe staining. Mito-Probe dye produces stronger fluorescence when staining the normal mitochondria than the permeabilized ones that are often found in apoptotic cells (28), whereas annexin V stains phosphatidylserine in the outer leaflet of the plasma membranes of apoptotic cells. Significant increases in macrophage apoptosis in the preparations from PLC β3–null mice were detected by both staining methods (Figure 2, B and C, and Supplemental Figure 2, A–D). We also measured caspase-3 activity and found that PLC β3–deficient macrophages also had significantly higher caspase-3 activity than the wild-type cells (Figure 2D). All of these observations suggest that PLC β3 signaling is involved in regulation of macrophage apoptosis. However, when macrophages isolated from mouse peritonea after 1-day thioglycolate elicitation were examined, we found no significant differences in macrophage apoptosis as measured by Mito-Probe (Figure 2E) or annexin V staining (data not shown). Together with the observations of no significant changes in either cell number or apoptosis of monocytes in the peripheral blood, spleen, and bone marrow (data not shown), we hypothesize that the lack of PLC β3 may not normally affect macrophage/monocyte apoptosis; rather it may render the macrophages more sensitive to apoptotic inducers that may become more abundant in 3-day than 1-day thioglycolate–elicited peritonea.

To test this possibility, we examined sensitivity of 1-day thioglycolate-elicited peritoneal macrophages to a number of apoptosis inducers. Oxysterols, components of oxLDL, are potent inducers of macrophage apoptosis (29–31). Treatment of wild-type macrophages with 25-OHC, an oxysterol, resulted in an about 1-fold increase in the number of apoptotic macrophages, whereas treatment of PLC β3–null macrophages resulted in more than a 4-fold increase (Figure 2E). This hypersensitivity to 25-OHC–induced apoptosis could also be recapitulated in mouse macrophage–like

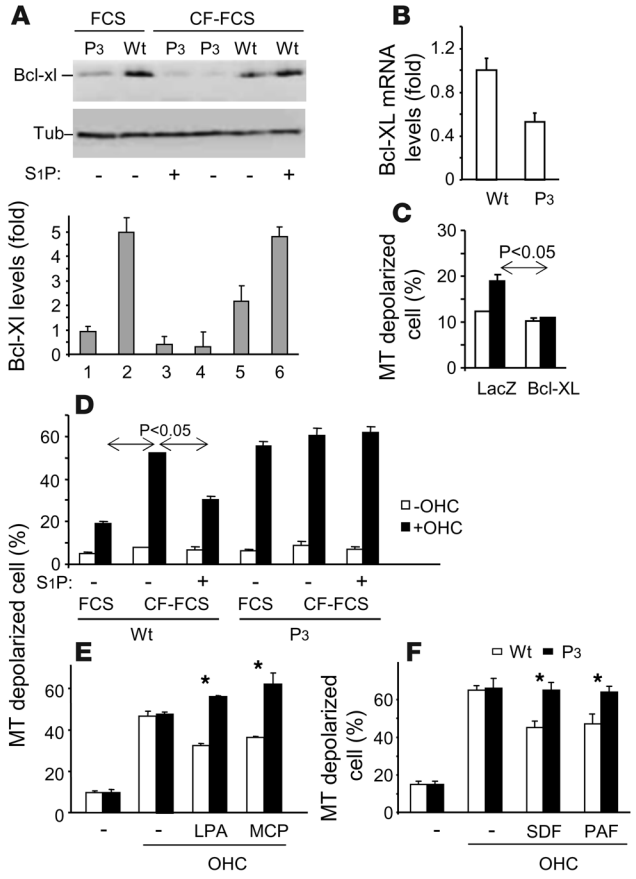

Figure 3
Ligand-induced PLC β3–dependent upregulation of Bcl-XL in macrophage and apoptosis protection. (**A**) One-day thioglycolate–elicited peritoneal macrophages were cultured in 10% FCS or charcoal-filtered FCS (CF-FCS) in the presence or absence of 300 nM S1P for 24 hours. Cells were then collected for Western blot analyses. Western blots from 3 experiments were quantified by densitometry. (**B**) Relative mRNA levels of Bcl-XL in 1-day thioglycolate–elicited peritoneal macrophages were determined by quantitative RT-PCR. (**C**) One-day thioglycolate–elicited PLC β3–null peritoneal macrophages were transfected with Bcl-XL expression plasmid using the Amaxa electroporation system. The next day, cells were treated with 25-OHC (2.5 μg/ml) for 24 hours and then stained with Mito-Probe. (**D**) Cells prepared and treated as in **A** were examined for their sensitivity to 25-OHC (10 μg/ml). (**E** and **F**) Cells prepared as in **A** were examined for their sensitivity to 25-OHC in the presence of 10% FCS or charcoal-filtered FCS containing SDF-1 (100 ng/ml), PAF (50 ng/ml), LPA (10 μM), or MCP (200 ng/ml). *$P < 0.05$ with versus without a ligand.

RAW264.7 cells, in which PLC β3 expression was suppressed by PLC β3–specific siRNA (Supplemental Figure 2, E and F), suggesting that this hypersensitivity is not a developmental effect of PLC β3 gene disruption. We also tested oxLDL, which was prepared following a previously described procedure (32). While our oxLDL preparation showed no effect on wild-type macrophages, it significantly enhanced the apoptosis of PLC β3–null macrophages (Figure 2F). While some investigators have reported that oxLDL promoted human and mouse macrophage apoptosis (30, 33), others have reported an opposite effect of oxLDL (34, 35). This discrepancy is likely due to different preparations of oxLDL, as lightly oxidized LDL may contain more antiapoptotic than proapoptotic components (36). Our oxLDL preparation may contain equal levels of anti- and proapoptotic components for wild-type cells, but the PLC β3–null cells may be more sensitive to the proapoptotic components, presumably including oxysterols. The combination of LPS or TNF-α with cycloheximide (CHX) has also been shown to stimulate macrophage apoptosis (37, 38). While LPS/CHX induced greater apoptosis of PLC β3–null macrophages than wild-type macrophages (Figure 2G), TNF-α/CHX did not (Figure 2H). All of these data together indicate that PLC β3 signaling may play a significant role in regulating macrophage sensitivity to apoptosis induction by some apoptosis inducers.

Because PLC β3 deficiency appears to affect mitochondrial potentials measured by the Mito-Probe dye, we hypothesize that PLC β3 signaling may regulate macrophage apoptosis via regulation of the levels and modifications of BH domain–containing proteins (39, 40). We compared the levels of p-Bad, Bad, Mcl-1, Bcl-2, Bok, Bim, Bik, Bmf, Bax, Bak, Puma, and Bcl-XL in the wild-type and PLC β3–null macrophages by using specific antibodies. We also examined the levels of p-Mapk, p-Akt, and p-65 NF-κB, which are also known to play important roles in cell survival (41–43). We did not observe any difference in the levels of these proteins in wild-type and PLC β3–null macrophages (data not shown) except for Bcl-XL. The level of Bcl-XL in wild-type macrophages was markedly higher than that in PLC β3–null cells (Figure 3A, compare lanes 1 and 2). Quantitative RT-PCR analysis revealed that this difference may be attributed at least in part to a higher Bcl-XL mRNA level in wild-type than PLC β3–null macrophages (Figure 3B). Bcl-XL belongs to the antiapoptotic BH domain–containing family of proteins, which also includes Bcl-2 and Mcl-1 (38). The reduction in Bcl-XL expression level in macrophages lacking PLC β3 would explain the hypersensitivity of these cells to apoptosis induction. The fact that exogenous expression of Bcl-XL in PLC β3–null peritoneal macrophages attenuated 25-OHC–induced apoptosis supports the explanation (Figure 3C).

As described earlier, a number of ligands are able to regulate PLC β3 in macrophages. These ligands are abundant in the serum and/or inflammatory tissues (44, 45). It is reasonable to hypothesize that these ligands may regulate Bcl-XL expression in macrophages via PLC β3. This hypothesis is supported by the finding that when the macrophages were cultured overnight in the presence of serum stripped by charcoal for removal of lipophilic ligands, such as S1P and LPA, the levels of Bcl-XL were markedly reduced compared with those in cells cultured in normal serum (Figure 3A, compare lanes 2 and 5). Importantly, when S1P was added back, it raised the Bcl-XL levels in wild-type macrophages back to those in cells cultured with normal serum, while failing to do so in cells lacking PLC β3 (Figure 3A). Consistent with what has been shown for the Bcl-XL levels, wild-type macrophages cultured in charcoal-stripped serum showed elevated sensitivity to 25-OHC–induced apoptosis, while PLC β3–null macrophages showed no significant difference (Figure 3D). Importantly, S1P treatment resulted in a significant reduction in 25-OHC–induced apoptosis of wild-type cells, but not PLC β3–null cells (Figure 3D). We also examined the effects of SDF-1, MCP-1, PAF, and LPA on macrophage sensitivity to 25-OHC–induced apoptosis. All of these ligands were able to protect wild-type macrophages, but not PLC β3–null macrophages (Figure 3, E and F), from 25-OHC–induced apoptosis to varying degrees. These ligands also

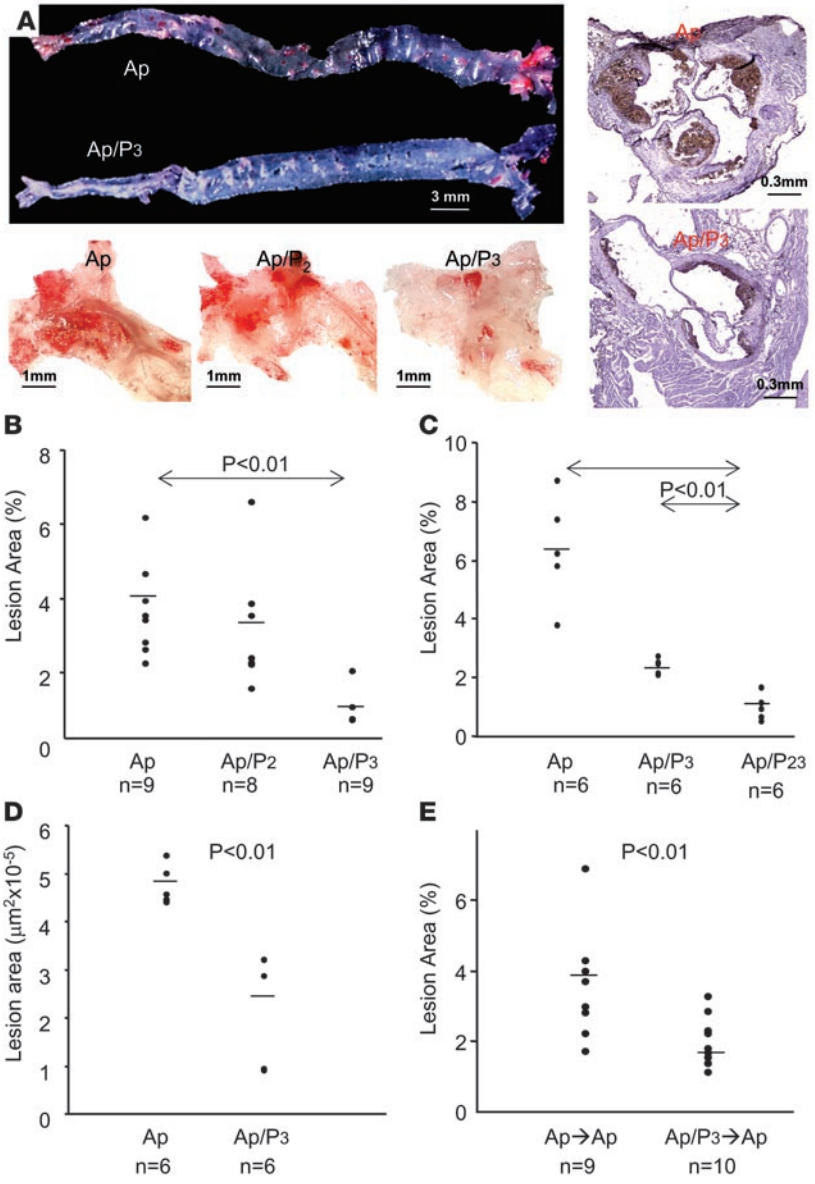

Figure 4

Decreased atherogenesis in mice lacking PLC β3. (**A**) Representative images of en face oil red O staining of spread aortas (top left panel) and aortic arches (bottom 3 left panels) and of Moma-2–stained cross sections of aortic roots (2 right panels) from apoE-null (Ap) and PLC β3/apoE–null (Ap/P_3) mice fed an HFD for 10 weeks. (**B**–**E**) Quantification of atherosclerotic lesion. apoE-null, PLC β2/apoE–null, and PLC β3/apoE–null mice fed an HFD for 10 weeks (**B**); apoE-null, PLC β3/apoE–null, and PLC β2/β3/apoE–null (Ap/P_{23}) mice fed a high-cholesterol diet for 17 weeks (**C** and **D**); and apoE-null mice receiving bone marrows from apoE-null or PLC β3/apoE–null mice fed an HFD for 14 weeks (**E**) were analyzed for lesion areas by en face staining of aortas (**B**, **C**, and **E**) or staining of cross sections of aortic roots with oil red O (**D**).

upregulated the levels of Bcl-XL (data not shown). Thus, PLC signaling is most likely to mediate multiple ligands in protection of macrophages from apoptosis induction in vivo.

Knowing that PLC β3–deficient macrophages are hypersensitive to apoptosis induction, particularly by 25-OHC and oxLDL, it is reasonable to hypothesize that PLC β3 deficiency would significantly impact the formation of atherosclerotic lesions, where oxLDL and oxysterols are enriched. Therefore, we decided to test PLC β deficiency in a mouse atherosclerosis model. Although it is anticipated that the lack of PLC β3 may increase macrophage apoptosis in the lesions, it is difficult to predict the outcome on atherogenesis itself because of the conflicting literature on the subject. There are reports showing a positive correlation between macrophage apoptosis and atherogenesis and ones showing the opposite (46–50). We favored the prediction that PLC β3 deficiency may be associated with a reduction in atherogenesis based on the finding that inactivation of Bax, which Bcl-XL counteracts, attenuated macrophage apoptosis and accelerated atherogenesis in a mouse model (48). Thus, we hoped that this atherosclerosis model study would not only provide a critical in vivo validation of what we have observed in isolated primary macrophages but also help to further clarify the role of macrophage apoptosis in atherogenesis. To investigate the effect of PLC β3 deficiency on atherogenesis, the PLC β3–null mice were first backcrossed to the C57BL background and then crossed with apoE-null mice, a well-established mouse atherosclerosis model (51, 52). The PLC β3/apoE–double-null mice, together with the apoE-null mice, were fed an HFD for 10 or 17 weeks. As shown in Figure 4A, PLC β3 deficiency led to marked reductions in atherosclerotic lesions in aortic vessels, arches, and roots compared with those in apoE-null mice. Quantification of lesion areas detected by en face oil red O staining of aortas revealed that there was a roughly 70% reduction in the lesion areas (Figure 4B). In addition, there were marked reductions in Moma-2 (a foam cell marker) staining at the aortic roots (Figure 4A). Serum lipid profiles of PLC β3/apoE–null mice were also compared with those of apoE-null mice; no significant differences in the levels of cholesterol, LDL, or triglyceride (Supplemental Figure 3A) were observed. A significant reduction (by 70%) in atherosclerotic lesion was also observed in PLC β3–null mice fed an HFD for 17 weeks when compared with apoE-null mice (Figure 4C). Lesions in aortic roots of these mice were also quantified; consistent with en face quantification, a significant reduction (by more than 50%) in the lesion was observed (Figure 4D). Once again, no significant changes in lipid profiles were found to be caused by PLC deficiency (Supplemental Figure 3B).

We also examined the effects of PLC β2 deficiency and PLC β2/β3 double deficiency on atherogenesis. PLC β2/apoE–double-knockout mice were generated by crossing PLC β2–null mice, which are also in the C57BL background, with apoE-null mice, and PLC β2/PLC β3/apoE–triple-knockout mice were subsequently generated by additional crossing. Although PLC β2 deficiency did not have a significant effect by itself (Figure 4, A and B), PLC β2/β3

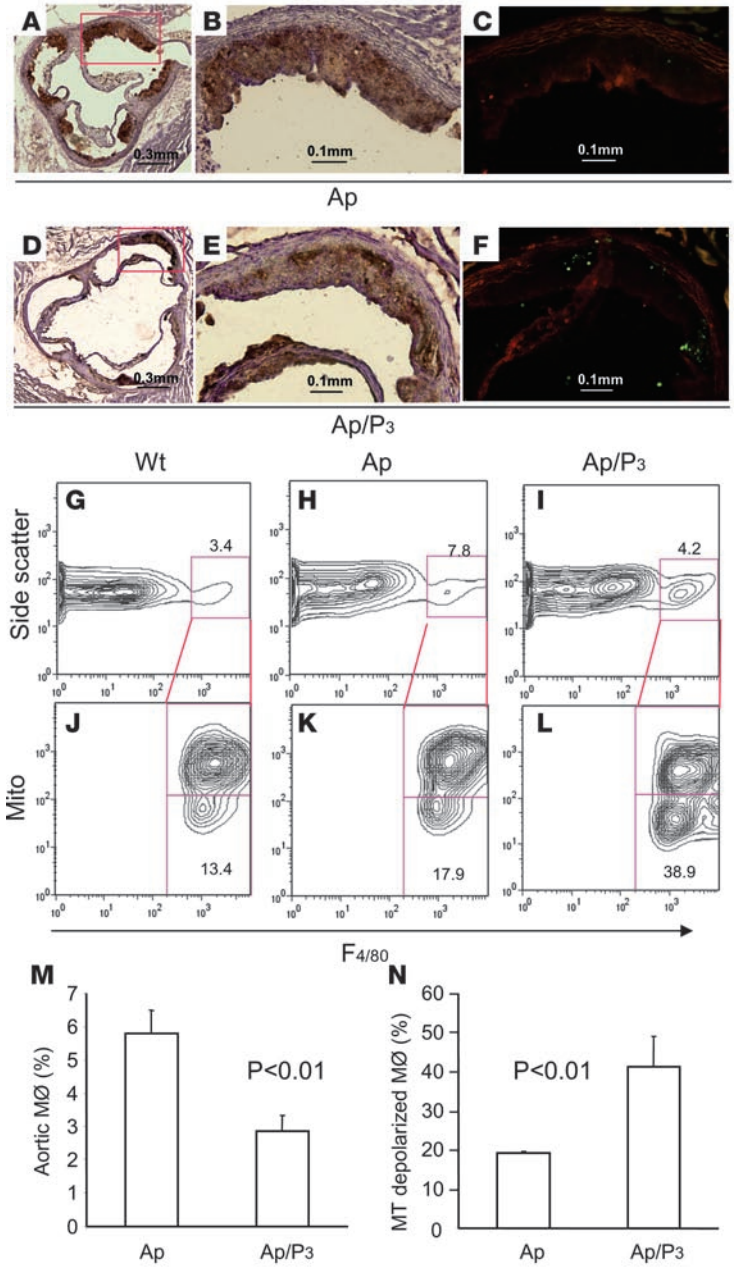

Figure 5

PLC β3 deficiency is associated with increased macrophage apoptosis in the atheromas. (**A**–**F**) Representative images of the cross sections of aortic roots from mice fed an HFD for 10 weeks stained with Moma-2 antibody (**A**, **B**, **D**, and **E**) or by TUNEL (**C** and **F**). **B** and **E** show magnifications of squared regions in **A** and **D**. **C** and **F** show adjacent sections of **B** and **E**, respectively. (**G**–**N**) Aortas from mice on an HFD for 17 weeks (**G**–**L**) or 10 weeks (*n* = 7; **M** and **N**) were analyzed for the number of macrophages and apoptotic macrophages.

double deficiencies resulted in a greater reduction in atherosclerotic lesion formation than PLC β3 deficiency did (Figure 4C). PLC β3 is widely expressed, but PLC β2 expression is relatively more restricted to hematopoietic cells. This synergistic effect of PLC β2 deficiency suggests that the lack of PLC in hematopoietic cells may contribute to the reduction in atherogenesis. In addition, these effects of PLC deficiencies on atherogenesis are consistent with their effects on ligand-induced Ca^{2+} effluxes in macrophages shown in Figure 1A, i.e., PLC β3 deficiency showed a greater effect than PLC β2 deficiency did, while PLC β2/β3 double deficiencies had the strongest effect. This correlation between the atherogenic phenotypes and Ca^{2+} efflux responses suggests that the effects of PLC deficiencies on atherogenesis may be attributed to their effects on macrophage functions.

To provide additional evidence for the lack of PLC β3 in hematopoietic cells being responsible for the atherogenic phenotypes of PLC β3 deficiency, we carried out adoptive bone marrow transfer experiments. Bone marrow cells from apoE-null and PLC β3/apoE–null mice were transferred to recipient apoE-null mice that had been lethally irradiated. As shown in Figure 4E, in mice that received PLC β3–null bone marrow cells, aortic lesions areas were more than 50% smaller than in mice that received cells expressing PLC β3. A similar result was seen in aortic root lesions (data not shown), and no difference in lipid profiles were noted (Supplemental Figure 3C). The bone marrow transplantation efficiency was verified by Western blot analysis of bone marrow cells using an anti–PLC β3 antibody; the PLC β3 protein was hardly detected in bone marrow cells isolated from mice that received PLC β3–null bone marrow (Supplemental Figure 3D). We also performed the transfer of apoE-null bone marrow cells to lethally irradiated apoE- and apoE/PLC β3–null recipients, respectively; no significant differences in their lesion areas were observed (Supplemental Figure 3E). All these results, together with the lack of effects of PLC β3 deficiency on chemokine-induced Ca^{2+} in spleen T and B cells (data not shown), indicate that PLC deficiency in hematopoietic cells, most likely macrophages, leads to a reduction in atherogenesis, which is in agreement with our hypothesis.

The next key question was whether PLC β3 deficiency increases macrophage apoptosis in atherosclerotic lesions. We first evaluated apoptosis in atherosclerotic lesions by staining adjacent sections of aortic roots from apoE-null and apoE/PLC β3–double-null mice with TUNEL and the anti–Moma-2 antibody, respectively (Figure 5, A–F, and Supplemental Figure 4). We found that there was more TUNEL-positive staining in the section from apoE/PLC β3–null mice than that from apoE-null mice (Figure 5, C and F), even though the lesion size of the apoE/PLC β3 sample was smaller (Figure 5, B and E). To carry out a more reliable and objective quantification of the number of macrophages and apoptotic macrophages in the lesions, we developed a FACS-based assay modified from a method reported by Ley's group (53). Cells dispersed from aortas of wild-type, apoE-null, and apoE/PLC β3–null mice (apoE- and apoE/PLC β3–null mice were on an HFD for 17 weeks) after collagenase A digestion were stained with the Mito-Probe dye and an anti-F4/80 antibody and subjected to FACS analysis. When compared with the wild-type samples, there was a marked increase in the number of macrophage (F4/80-positive) cells in the apoE-null samples (Figure 5, G and H). This is consistent with the current knowledge of increased infiltration of macrophages in atherosclerotic lesions. Importantly, the number of macrophages in the apoE/PLC β3–null sample was less than

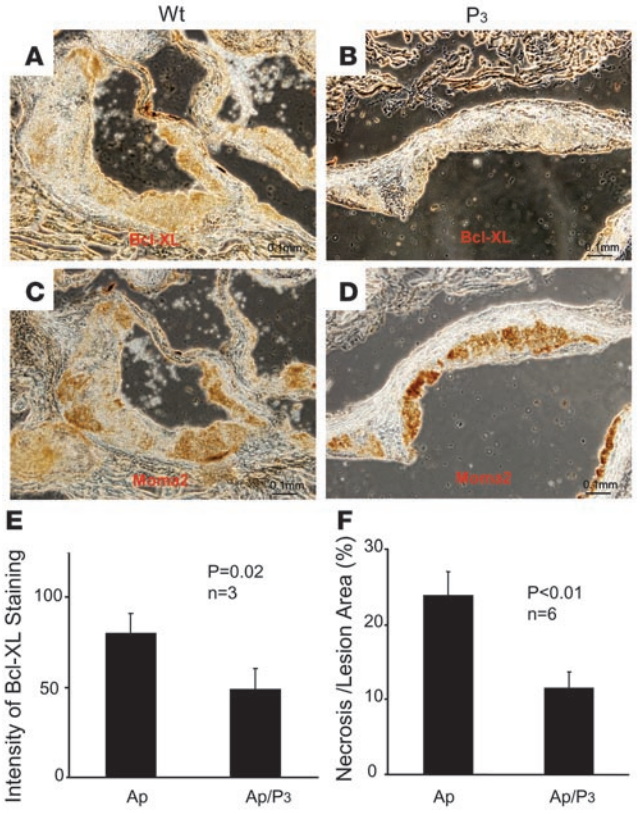

Figure 6
Effect of PLC β3 deficiency on BcL-XL expression in the lesions and on necrotic core size. Adjacent aortic root sections of apoE- (**A** and **C**) and apoE/PLC β3–null (**B** and **D**) mice fed an HFD were stained with an anti–Bcl-XL antibody in parallel (**A** and **B**) or the anti–Moma-2 antibody (**C** and **D**). (**E**) Quantification of Bcl-XL staining (n = 6). (**F**) The necrotic core size in aortic root sections from mice on an HFD for 17 weeks was quantified.

that in the apoE-null sample (Figure 5, H and I), but slightly more than that in the wild-type mouse (Figure 5, G and I). These results agree well with significant reduction in atherosclerotic lesions in the apoE/PLC β3–null mice (Figure 4). Even though the apoE/PLC β3–null sample had fewer macrophages than the apoE-null one, it had an increased percentage of F4/80-positive macrophages that were mitochondria depolarized compared to the one lacking only apoE (Figure 5, K and L). On the other hand, the proportion of apoptotic cells in the apoE-null aorta was just slightly higher than that in the wild-type aorta (Figure 5, compare K and J). These data suggest that there is a marked increase in the apoptosis of PLC β3–null macrophages in the aortic lesions, which is correlated with a reduction in atherogenesis. We analyzed another set of wild-type, PLC β3/apoE–null, and apoE-null samples from mice on an HFD for 17 weeks, and the results were the same (data not shown). To obtain statistical analysis, we carried out a similar experiment using 7 pairs of apoE- and apoE/PLC β3–null mice fed an HFD for 10 weeks. The results, which are shown in Figure 5, M and N, were the essentially same. To examine whether there are differences in the Bcl-XL expression levels between the wild-type and PLC β3–null lesion areas, we stained aortic root sections with an anti–Bcl-XL antibody. Significant differences in Bcl-XL staining between the wild-type and PLC β3–null sections were observed (Figure 6, A–E). We also stained the adjacent sections with the anti–Moma-2 antibody. Bcl-XL was readily detected in the macrophages in the lesions from the wild-type mice. We also quantified the necrosis in the lesions of mice fed an HFD for 17 weeks. There was less necrosis in lesions from PLC β3–null mice than those from the wild-type mice (Figure 6F). Therefore, we conclude that PLC β3 deficiency is associated with a significant increase in apoptotic macrophages in atherosclerotic lesions, probably as the result of reduction in Bcl-XL levels, which in turn contributes to the reduction in the number of macrophages in the lesions as well as the lesion size.

Discussion

Our work has demonstrated that PLC β3, a major functional PLC isoform that is activated by a number of G protein–coupled ligands in macrophages, plays an important role in regulating macrophage sensitivity to apoptotic induction by oxysterols and LPS. PLC signaling regulates the sensitivity at least in part by regulating the expression of Bcl-XL. We subsequently validated the in vivo significance of this PLC β3–mediated mechanism in a mouse atherosclerosis model. In this model study, we found that PLC β3 deficiency was associated with significant reductions in atherogenesis and increases in macrophage apoptosis in atherosclerotic lesions and sensitivity to apoptotic induction in vitro.

It is well accepted that chemokines and their receptors have important roles in atherogenesis (9, 11–13), and these roles of chemokines have been largely attributed to their regulation of macrophage recruitment. The finding that SDF-1 and, to a lesser extent, MCP-1 can protect macrophages from apoptosis induction, however, suggests that chemokines may regulate atherogenesis via diverse mechanisms. While S1P and LPA can activate PLC via both the Gq and Gi family of proteins, chemokines including both MCP-1 and SDF-1 activate PLC primarily via the Gi proteins in leukocytes (54–56). PLC β3 was shown to be activated by both the Gα subunits of the Gq family and Gβγ subunits. Thus, it is reasonable to observe that all these ligands are able protect macrophages from apoptotic induction in a PLC β3–dependent manner. It also appears that PKC has an important role in PLC β3–mediated regulation of macrophage apoptosis, as a PKC inhibitor, Go6976, inhibited serum-mediated protection of macrophage apoptosis induced by 25-OHC (data not shown).

It is also important to note that PLC β3 deficiency did not by itself cause excessive cell death of either macrophages (Figure 1E) or monocytes (data not shown), nor did it alter the numbers or apoptotic levels of monocytes in the spleen, bone marrow, and circulation even in the apoE-null background. These observations suggest that this PLC signaling–mediated antiapoptotic mechanism may either be specific for macrophages or function under a specific context where PLC-activating ligands and proapoptotic stimuli are enriched. Thus, it is reasonable to find that this mechanism is highly relevant in the atherosclerotic lesions, in which both apoptotic inducers (oxysterols) and PLC-activating ligands (chemokines, S1P, LPA, and PAF) are abundantly present. It is conceivable to postulate that macrophages develop this protective mechanism to cope with harsh environments these cells often encounter as the primary scavenger cells. Such harsh environments are presumably found in inflammation and microbial infections. Although this protective mechanism, particularly the resistance

to LPS-induced apoptosis (Figure 2G), may be beneficial in antimicrobial actions and even acute inflammation, the mechanism appears to be counterproductive during atherogenesis and maybe other chronic inflammatory conditions. Thus, it is of great interests to investigate the significance of PLC β3 signaling in other inflammation-related paradigms.

The roles of macrophage apoptosis in atherogenesis have been investigated in a number of recent studies. It seems that macrophage apoptosis may show different effects on atherogenesis depending on the stages at which it occurs. An increase in macrophage apoptosis in early lesions appears to cause the attenuation of atherogenesis, whereas impairment in macrophage apoptosis in late lesions may contribute to necrosis, leading to increased proinflammatory responses and atherogenesis (47–50, 57, 58). Given that there is no increase in necrotic core size associated with PLC β3 deficiency, our results are consistent with the idea that the lack of PLC β3 enhances the sensitivity of newly recruited macrophages to 25-OHC– or oxLDL-induced apoptosis in early atherosclerotic lesions, which causes them to decease before they become foam cells, the building blocks for atherosclerotic plaques. Fewer foam cells would mean smaller lesions. However, because of the early lesion suppression by PLC β3 deficiency, it is difficult to draw any conclusion on the direct effect of the PLC signaling–regulated macrophage apoptosis on advanced lesion progression. This issue may have to be addressed by temporal or pharmacological control of PLC β3 expression in future. Although we have not found any effect of PLC β3 deficiency on the macrophage activities other than apoptosis, our present study also cannot completely exclude the possibility that some unknown macrophage functions mediated by this PLC pathway contribute to the atherogenic phenotypes. Nevertheless, our study has established a clear correlation between the absence of PLC β3 on the one hand and an increase in macrophage apoptosis and reduction in atherogenesis on the other. Although we have only studied mouse macrophages, recent work showing that S1P induced upregulation of Bcl-XL and Bcl-2 in human macrophages and protected human macrophages from apoptosis induction (38) provides the possible relevance for our study for humans. Together with the fact that PLC β3 deficiency is associated with no apparent gross phenotypes, we believe that PLC β3 may be a potential antiatherosclerosis target.

Methods

Animals. PLC β2–null and PLC β3–null mice were backcrossed with C57BL/6J mice for more than 10 generations. These mice were then crossed with each other to produce PLC β2/β3–null mice and with apoE-null mice in the C57BL/6J background purchased from the Jackson Laboratory (Apoetm1Unc/J). For analysis of atherogenesis, mice were fed an HFD (Harlan Teklad) starting at 5 weeks of age for 10 or 17 weeks. All animal procedures used in this study followed institutional guidelines of the University of Connecticut Health Center and Yale University and were approved by the University of Connecticut Health Center Animal Care Committee and the Yale University Institutional Animal Care and Use Committee.

Cells, plasmids, chemoattractants, and antibodies. Raw264.7 cells were cultured in DMEM (Cellgro) supplemented with 10% FCS (Hyclone; heat-inactivated), penicillin and streptomycin. Raw264.7 cells were transfected using Lipofectamine (Invitrogen). Expression plasmids for LacZ, PAK1, and the kinase-dead mutant of PAK1 were described previously (59).

Peritoneal macrophages were prepared 24 hours or 72 hours after mice were injected with 1 ml of 3% thioglycolate broth (Sigma-Aldrich). Peritoneal cavities were lavaged with 10 ml HBSS (Gibco; Invitrogen), and an aliquot of cells was stained with the anti-F4/80 antibody. Generally, 90% of the cells isolated after 72 hours were F4/80 positive, and more than 60% were F4/80 positive after 24-hour induction.

SDF-1 and MCP-1 were purchased from PeproTech Inc. C5a was purchased from Sigma-Aldrich. Anti–Bcl-XL antibody and anti-PAK1 antibodies were purchased from Cell Signaling Technology Inc. Anti–phospho-JNK antibody was purchased from United Biomedical Inc. Anti–Moma-2 antibody was purchased from Serotec Inc. CD11b and Gr-1 antibody were purchased from BD Biosciences — Pharmingen. F4/80 antibody was purchased from Serotec Inc.

Calcium efflux assay. Peritoneal macrophages of WT and PLC β2–, PLC β3–, and PLC β2/β3–null mice were collected and labeled with Fluo-3. Cell suspensions were collected in a flow cytometer for 30 seconds before the C5a was added into suspension. Calcium intensity was recorded in real time.

Macrophage apoptosis assays. To analyze macrophage apoptosis, cells were stained with annexin V and propidium iodide using the ApoAlert AnnexinV-FITC Apoptosis Kit (Clontech) or with Mito-Probe DiIC1 dye (Invitrogen), and the anti-F4/80 antibody and analyzed by FACS. The caspase activity assays were performed using a Homogeneous Caspase Assay from Roche based on the manufacturer's suggested protocol.

To test macrophages' sensitivity to 25-OHC or oxLDL, cells were incubated with or without 10 μg/ml 25-hydroxycholesterol (Sigma-Aldrich) or 100 μg/ml oxLDL in DMEM containing 10% FCS for 24 hours at 37°C and analyzed for apoptosis. For examination of the effects of S1P, cells were resuspended in DMEM containing 10% charcoal-filtered FCS (Gemini Bio-Products) and treated with or without 300 nM S1P in the presence or absence of 10 μg/ml 25-OHC. Cells were analyzed for apoptosis 24 hours later.

For analysis of Raw264.7 cells, the cells that were transfected for 24 hours were incubated with 30 μg/ml 25-OHC for an additional 24 hours before they were analyzed by FACS with the Mito-Probe dye.

Quantification of macrophage number and apoptosis in aortas. Aortas were quickly dissected as described in *Atherosclerotic lesion analysis*, and were minced and incubated with 1 mg/ml collagenase A (Roche) for 2 hours at 37°C. Then, the cells were gently spun down and stained with the anti-F4/80 antibody and Mito-Probe dye and analyzed by FACS.

Sample preparation for Western blot analysis. Peritoneal macrophages were cultured in DMEM containing 10% charcoal-filtered or normal FCS in the presence or absence of 10 μg/ml 25-OHC or 300 nM S1P for 24 hours at 37°C before being directly lysed with the SDS-PAGE sample buffer.

Cell migration assays. Cell migration assays were performed using 24-well Transwell plates (5-μm pore size; Costar). Two million peritoneal macrophages or 5 million spleen cells were loaded into the upper chambers. The lower chambers were filled with medium (DMEM plus 1% FCS) in the absence or presence of chemoattractants. In some experiments, Transwell inserts were cultured with a layer of mouse embryonic immortalized endothelial cells (60). Transwell plates were then incubated at 37°C for 4 hours. For peritoneal macrophage migration assays, cells attached to the lower surfaces of inserts were trypsinized and collected for counting and FACS analysis after staining with the anti-F4/80 antibody. For quantification of spleen monocyte migration, cells in the lower chambers were collected for counting and FACS analysis after being stained with anti-CD11b and anti–Gr-1 antibodies. The number of monocytes was determined based on the total migrated cell number and percentage of monocytes ($CD11b^{mid}$ and $Gr\text{-}1^{lo}CD11b^{mid}$).

Adhesion assay. Five million spleen cells were added into tissue culture plates (Costar) without coating or precoated with 50 μg/ml poly-lysine, 1 μg/ml fibronectin (Sigma-Aldrich), or a layer of mouse endothelial

cells. The plates were then incubated in 37°C for 10 minutes. After cells were washed with PBS 5 times, adherent cells were detached by trypsinization, counted, and analyzed by FACS after staining with anti-CD11b and anti–Gr-1 antibodies.

Phagocytosis assay. Peritoneal macrophages were seeded to culture plates for 3 hours at 37°C. Uncoated FluoSphere beads (Molecular Probes; Invitrogen) and those coated with oxLDL were added to the cultures after unattached cells were rinsed away. After 10 minutes of incubation at 37°C, excessive beads were washed away, and the macrophages were detached by trypsinization and analyzed by FACS after being stained with the anti-F4/80 antibody.

For the phagocytosis assay of apoptotic Jurkat cells, the apoptosis was induced by incubating Jurkat cells with an anti-Fas antibody (Upstate) for 6 hours in 37°C. Apoptosis was verified by annexin V/propidium iodide staining. Apoptotic Jurkat cells were then labeled with Vybrant CFDA SE (Molecular Probes; Invitrogen) and added to peritoneal macrophages. After 3 hours of incubation at 37°C, the unbounded Jurkat cells were washed away before macrophages were detached and stained with F4/80. The cells were analyzed by a flow cytometer. The mean fluorescence intensity of CFDA SE gated for F4/80-positive cells is shown as the number of apoptotic Jurkat cells associated with macrophages.

Atherosclerotic lesion analysis. Mice were anesthetized, and blood samples were collected via heart puncture for lipid profile analyses (total cholesterol, LDL, HDL, and triglycerides by IDEXX Veterinarian Laboratories). Then the cardiovascular system was perfused with 20 ml 1× DPBS (Cellgro), through the heart apex, followed by 5 ml fixatives (4% PFA, 5% sucrose, 20 μM EDTA in 1× DPBS, pH 7.4). The aorta from the aortic root to iliac artery was dissected and cut open longitudinally in situ and immerged in the fixative for 12 hours before being rinsed with 1× PBS and stained with oil red O (Fisher Biotech). The aorta was then spread, and the lesion area was quantified using the imaging analysis software ImagePro from Media Cybernetics. The heart and proximal portion of aortic root were also fixed and embedded in OCT for lesion area quantification on cross sections of the aortic root, as previously described (61).

Bone marrow transplantation. Recipient apoE-null mice were lethally irradiated with 5.50 Gy twice at a 4-hour interval. Twenty four hours later, the mice were transplanted via tail vein injection with bone marrow cells (2 million/recipient) from apoE-null mice or apoE/PLC β3–null mice. The bone marrow cells were prepared by flushing femurs with 1× DPBS and lysing red blood cells with rbc lysis buffer (8.3 g NH_4Cl, 1.0 g $KHCO_3$, 1.8 ml 5% EDTA in 1,000 ml dH_2O). Four weeks after bone marrow transfer, recipient mice were fed an HFD for 10 weeks for atherosclerotic lesion analysis. Before mice were euthanized, bone marrow cells were collected for Western blot detection of PLC β3 protein to monitor transplantation efficiency.

Immunohistochemistry and TUNEL staining. For Moma-2 and Bcl-XL staining, frozen sections were fixed with acetone/methanol (vol/vol 1:1) for 30 minutes before being transferred to 1× TBS (8.766 g/l NaCl, 6.055 g/l Tris, pH 7.4) for 10 minutes at room temperature. Sections were then immersed in 0.3% H_2O_2, rinsed, and transferred into 10% normal rabbit serum (Vector Laboratories), followed by staining with rat anti-mouse Moma-2 antibody, biotinylated second antibody, and HRP-avidin conjugates using the ABC kit from Vector Laboratories. Finally, the sections were developed with DAB (Dako North American), and some of the sections were counterstained with hematoxylin (Thermo Electron Corp.). Bcl-XL staining intensity was quantified by using MetaMorph software in circumscribed areas of atherosclerotic lesions.

For TUNEL staining, the sections were stained with the TACS In Situ Kit (R&D Systems) based on the manufacturer's suggestions. Briefly, sections were immerged in PBS for 15 minutes at room temperature, incubated with protease K for 15 minutes at room temperature, transferred into the TdT labeling buffer, and incubated with the TdT labeling reaction mix. Labeling was stopped by transferring sections to the stop buffer, and the sections were incubated in Strep-Fluor. All reagents were provided in the kit.

Expression of Bcl-XL in primary macrophages. Macrophages isolated from mouse peritonea were cotransfected with the EGFP and Bcl-XL expression plasmids at a ratio of 1:2 using the Amaxa electroporation system. Twenty-four hours after transfection, cells were collected and treated with 25-OHC, stained with the Mito-Probe dye, and analyzed by a flow cytometer as described above. The GFP-positive cell population was gated in the analysis of apoptosis. The transfection efficiency was around 10%. The control group was primary macrophages transfected with EGFP plus LacZ.

Quantitative RT-PCR. Total RNA was isolated from macrophages of WT and PLC β3–null mice using TRIzol reagent (Invitrogen) according to the manufacturer's instructions. For quantitative PCR analysis, RNA was reverse transcribed using the iScript cDNA synthesis kit (Bio-Rad). Quantitative PCR was carried out using the QuantiTect SYBR Green PCR kit (QIAGEN) on a DNA Engine OPTICON (MJ Research Inc.) instrument. β-Actin was used as an internal reference for each sample. Using a formula previously described (62), the relative change in mRNA levels was normalized against the β-actin mRNA levels. The sense primer was 5′-CTGTGCGTGGAAAGCGTAGA-3′, and the antisense primer was 5′-GTCAGGAACCAGCGGTTGAA-3′.

PLC β3 siRNA expression in RAW264.7 cells. RAW264.7 cells were transfected with either pAS control vector or pAS–PLC β3 by using Lipofectamine reagent (Invitrogen). Forty-eight hours after transfection, the cells were collected and treated with 25-OHC and analyzed for apoptosis as described above. During analysis, only the GFP-positive cell population was gated in the analysis of apoptosis.

Quantification of necrotic core size. A modification of a previously described method (49) was performed to measure necrosis in atherosclerotic lesions. The frozen tissue blocks were placed on a cryotome, and 6-μm serial sections of the ascending aorta were collected on coated glass slides until the most cranial portion of the aortic sinus could be identified by examining unstained sections. Once the first section was identified, the 36 cranial sections, covering 216 μm of the ascending aorta, were used for further evaluation. Every twelfth section of the ascending aorta was stained with H&E. The necrosis areas were circumscribed by using MetaMorph software (Molecular Devices) based on characteristic morphologic features of necrosis. The area of necrosis of each slide was calculated and normalized to the total lesion area.

Statistics. For atherosclerotic lesion area analysis, both 2-tailed Student's *t* test and Mann-Whitney *U* test were performed. The *P* values generated by both analyses were consistent. For the rest of the assays, Student's *t* test was used to calculate the statistical significance. $P < 0.05$ was considered significant.

Acknowledgments

We thank Linglin Tang and Wenzhong Liu for technical help. The work was supported by NIH grants.

Received for publication June 29, 2007, and accepted in revised form October 17, 2007.

Address correspondence to: Dianqing Wu, Department of Pharmacology, Yale University School of Medicine, 333 Cedar St., New Haven, Connecticut 06520-8066, USA. Phone: (203) 785-3149; Fax: (203) 737-1097; E-mail: dan.wu@yale.edu.

1. Berridge, M.J. 1989. Inositol phosphates and cell signaling. *Nature.* **341**:197–205.
2. Rhee, S.G., and Bae, Y.S. 1997. Regulation of phosphoinositide-specific phospholipase C isozymes. *J. Biol. Chem.* **272**:15045–15048.
3. Jiang, H.P., et al. 1996. Phospholipase C b4 is involved in modulating the visual response in mice. *Proc. Natl. Acad. Sci. U. S. A.* **93**:14598–14601.
4. Kano, M., et al. 1998. Phospholipase Cbeta4 is specifically involved in climbing fiber synapse elimination in the developing cerebellum. *Proc. Natl. Acad. Sci. U. S. A.* **95**:15724–15729.
5. Wu, D., Huang, C., and Jiang, H. 2000. Roles of phospholipid signaling in chemoattractant-induced responses. *J. Cell Sci.* **113**:2935–2940.
6. Mosser, D.M. 2003. The many faces of macrophage activation. *J. Leukoc. Biol.* **73**:209–212.
7. Stout, R.D., and Suttles, J. 2004. Functional plasticity of macrophages: reversible adaptation to changing microenvironments. *J. Leukoc. Biol.* **76**:509–513.
8. Reape, T.J., and Groot, P.H. 1999. Chemokines and atherosclerosis. *Atherosclerosis.* **147**:213–225.
9. Charo, I.F., and Ransohoff, R.M. 2006. The many roles of chemokines and chemokine receptors in inflammation. *N. Engl. J. Med.* **354**:610–621.
10. Boisvert, W.A. 2004. Modulation of atherogenesis by chemokines. *Trends Cardiovasc. Med.* **14**:161–165.
11. Libby, P. 2002. Inflammation in atherosclerosis. *Nature.* **420**:868–874.
12. Kraaijeveld, A.O., de Jager, S.C., van Berkel, T.J., Biessen, E.A., and Jukema, J.W. 2007. Chemokines and atherosclerotic plaque progression: towards therapeutic targeting? *Curr. Pharm. Des.* **13**:1039–1052.
13. Gerszten, R.E., Mach, F., Sauty, A., Rosenzweig, A., and Luster, A.D. 2000. Chemokines, leukocytes, and atherosclerosis. *J. Lab. Clin. Med.* **136**:87–92.
14. Boring, L., Gosling, J., Cleary, M., and Charo, I.F. 1998. Decreased lesion formation in CCR2$^{-/-}$ mice reveals a role for chemokines in the initiation of atherosclerosis. *Nature.* **394**:894–897.
15. Dawson, T.C., Kuziel, W.A., Osahar, T.A., and Maeda, N. 1999. Absence of CC chemokine receptor-2 reduces atherosclerosis in apolipoprotein E-deficient mice. *Atherosclerosis.* **143**:205–211.
16. Boring, L., et al. 1997. Impaired monocyte migration and reduced type 1 (Th1) cytokine responses in C-C chemokine receptor 2 knockout mice. *J. Clin. Invest.* **100**:2552–2561.
17. Kurihara, T., Warr, G., Loy, J., and Bravo, R. 1997. Defects in macrophage recruitment and host defense in mice lacking the CCR2 chemokine receptor. *J. Exp. Med.* **186**:1757–1762.
18. Kuziel, W.A., et al. 1997. Severe reduction in leukocyte adhesion and monocyte extravasation in mice deficient in CC chemokine receptor 2. *Proc. Natl. Acad. Sci. U. S. A.* **94**:12053–12058.
19. Gu, L., et al. 1998. Absence of monocyte chemoattractant protein-1 reduces atherosclerosis in low density lipoprotein receptor-deficient mice. *Mol. Cell.* **2**:275–281.
20. Gosling, J., et al. 1999. MCP-1 deficiency reduces susceptibility to atherosclerosis in mice that overexpress human apolipoprotein B. *J. Clin. Invest.* **103**:773–778.
21. Aiello, R.J., et al. 1999. Monocyte chemoattractant protein-1 accelerates atherosclerosis in apolipoprotein E-deficient mice. *Arterioscler. Thromb. Vasc. Biol.* **19**:1518–1525.
22. Chang, J.D., et al. 2007. Deletion of the phosphoinositide 3-kinase p110gamma gene attenuates murine atherosclerosis. *Proc. Natl. Acad. Sci. U. S. A.* **104**:8077–8082.
23. Gerard, C., and Rollins, B.J. 2001. Chemokines and disease. *Nat. Immunol.* **2**:108–115.
24. Rossi, D., and Zlotnik, A. 2000. The biology of chemokines and their receptors. *Annu. Rev. Immunol.* **18**:217–242.
25. Wu, D. 2005. Signaling mechanisms for regulation of chemotaxis. *Cell Res.* **15**:52–56.
26. Jiang, H., et al. 1997. Roles of phospholipase C beta2 in chemoattractant-elicited responses. *Proc. Natl. Acad. Sci. U. S. A.* **94**:7971–7975.
27. Li, Z., et al. 2000. Roles of PLC-beta2 and -beta3 and PI3Kgamma in chemoattractant-mediated signal transduction. *Science.* **287**:1046–1049.
28. Han, J., Goldstein, L.A., Gastman, B.R., and Rabinowich, H. 2006. Interrelated roles for Mcl-1 and BIM in regulation of TRAIL-mediated mitochondrial apoptosis. *J. Biol. Chem.* **281**:10153–10163.
29. Brown, A.J., and Jessup, W. 1999. Oxysterols and atherosclerosis. *Atherosclerosis.* **142**:1–28.
30. Colles, S.M., Maxson, J.M., Carlson, S.G., and Chisolm, G.M. 2001. Oxidized LDL-induced injury and apoptosis in atherosclerosis. Potential roles for oxysterols. *Trends Cardiovasc. Med.* **11**:131–138.
31. Panini, S.R., and Sinensky, M.S. 2001. Mechanisms of oxysterol-induced apoptosis. *Curr. Opin. Lipidol.* **12**:529–533.
32. Calvo, D., Gomez-Coronado, D., Suarez, Y., Lasuncion, M.A., and Vega, M.A. 1998. Human CD36 is a high affinity receptor for the native lipoproteins HDL, LDL, and VLDL. *J. Lipid Res.* **39**:777–788.
33. Salvayre, R., Auge, N., Benoist, H., and Negre-Salvayre, A. 2002. Oxidized low-density lipoprotein-induced apoptosis. *Biochim. Biophys. Acta.* **1585**:213–221.
34. Hundal, R.S., et al. 2003. Oxidized low density lipoprotein inhibits macrophage apoptosis by blocking ceramide generation, thereby maintaining protein kinase B activation and Bcl-XL levels. *J. Biol. Chem.* **278**:24399–24408.
35. Hamilton, J.A., Jessup, W., Brown, A.J., and Whitty, G. 2001. Enhancement of macrophage survival and DNA synthesis by oxidized-low-density-lipoprotein (LDL)-derived lipids and by aggregates of lightly oxidized LDL. *Biochem. J.* **355**:207–214.
36. Boullier, A., et al. 2006. Minimally oxidized LDL offsets the apoptotic effects of extensively oxidized LDL and free cholesterol in macrophages. *Arterioscler. Thromb. Vasc. Biol.* **26**:1169–1176.
37. Suzuki, T., et al. 2004. Mechanisms involved in apoptosis of human macrophages induced by lipopolysaccharide from Actinobacillus actinomycetemcomitans in the presence of cycloheximide. *Infect. Immun.* **72**:1856–1865.
38. Weigert, A., et al. 2006. Apoptotic cells promote macrophage survival by releasing the anti-apoptotic mediator sphingosine-1-phosphate. *Blood.* **108**:1635–1642.
39. Gross, A., McDonnell, J.M., and Korsmeyer, S.J. 1999. BCL-2 family members and the mitochondria in apoptosis. *Genes Dev.* **13**:1899–1911.
40. Kim, H., et al. 2006. Hierarchical regulation of mitochondrion-dependent apoptosis by BCL-2 subfamilies. *Nat. Cell Biol.* **8**:1348–1358.
41. Karin, M. 2006. Nuclear factor-kappaB in cancer development and progression. *Nature.* **441**:431–436.
42. Letai, A. 2006. Growth factor withdrawal and apoptosis: the middle game. *Mol. Cell.* **21**:728–730.
43. Xia, Z., Dickens, M., Raingeaud, J., Davis, R.J., and Greenberg, M.E. 1995. Opposing effects of ERK and JNK-p38 MAP kinases on apoptosis. *Science.* **270**:1326–1331.
44. Hla, T. 2004. Physiological and pathological actions of sphingosine 1-phosphate. *Semin. Cell Dev. Biol.* **15**:513–520.
45. Lee, H., Liao, J.J., Graeler, M., Huang, M.C., and Goetzl, E.J. 2002. Lysophospholipid regulation of mononuclear phagocytes. *Biochim. Biophys. Acta.* **1582**:175–177.
46. Geng, Y.J., and Libby, P. 2002. Progression of atheroma: a struggle between death and procreation. *Arterioscler. Thromb. Vasc. Biol.* **22**:1370–1380.
47. Arai, S., et al. 2005. A role for the apoptosis inhibitory factor AIM/Spalpha/Api6 in atherosclerosis development. *Cell Metab.* **1**:201–213.
48. Liu, J., et al. 2005. Reduced macrophage apoptosis is associated with accelerated atherosclerosis in low-density lipoprotein receptor-null mice. *Arterioscler. Thromb. Vasc. Biol.* **25**:174–179.
49. Han, S., et al. 2006. Macrophage insulin receptor deficiency increases ER stress-induced apoptosis and necrotic core formation in advanced atherosclerotic lesions. *Cell Metab.* **3**:257–266.
50. Baldan, A., et al. 2006. Impaired development of atherosclerosis in hyperlipidemic Ldlr$^{-/-}$ and ApoE$^{-/-}$ mice transplanted with Abcg1$^{-/-}$ bone marrow. *Arterioscler. Thromb. Vasc. Biol.* **26**:2301–2307.
51. Plump, A.S., et al. 1992. Severe hypercholesterolemia and atherosclerosis in apolipoprotein E-deficient mice created by homologous recombination in ES cells. *Cell.* **71**:343–353.
52. Zhang, S.H., Reddick, R.L., Piedrahita, J.A., and Maeda, N. 1992. Spontaneous hypercholesterolemia and arterial lesions in mice lacking apolipoprotein E. *Science.* **258**:468–471.
53. Galkina, E., et al. 2006. Lymphocyte recruitment into the aortic wall before and during development of atherosclerosis is partially L-selectin dependent. *J. Exp. Med.* **203**:1273–1282.
54. Sanchez, T., and Hla, T. 2004. Structural and functional characteristics of S1P receptors. *J. Cell. Biochem.* **92**:913–922.
55. Locati, M., and Murphy, P.M. 1999. Chemokines and chemokine receptors: biology and clinical relevance in inflammation and AIDS. *Annu. Rev. Med.* **50**:425–440.
56. Anliker, B., and Chun, J. 2004. Cell surface receptors in lysophospholipid signaling. *Semin. Cell Dev. Biol.* **15**:457–465.
57. Tabas, I. 2005. Consequences and therapeutic implications of macrophage apoptosis in atherosclerosis: the importance of lesion stage and phagocytic efficiency. *Arterioscler. Thromb. Vasc. Biol.* **25**:2255–2264.
58. Schrijvers, D.M., De Meyer, G.R., Herman, A.G., and Martinet, W. 2007. Phagocytosis in atherosclerosis: molecular mechanisms and implications for plaque progression and stability. *Cardiovasc. Res.* **73**:470–480.
59. Li, Z., et al. 2003. Directional sensing requires G beta gamma-mediated PAK1 and PIX alpha-dependent activation of Cdc42. *Cell.* **114**:215–227.
60. Paik, J.H., et al. 2004. Sphingosine 1-phosphate receptor regulation of N-cadherin mediates vascular stabilization. *Genes Dev.* **18**:2392–2403.
61. Baglione, J., and Smith, J.D. 2006. Quantitative assay for mouse atherosclerosis in the aortic root. *Methods Mol. Med.* **129**:83–95.
62. Pfaffl, M.W. 2001. A new mathematical model for relative quantification in real-time RT-PCR. *Nucleic Acids Res.* **29**:e45.